1-20-2003

The system parameters of DW Ursae Majoris

S. Araujo-Betancor
University of Southampton

C. Knigge
University of Southampton

K. S. Long
Space Telescope Science Institute

D. W. Hoard
California Institute of Technology

P. Szkody
University of Washington

See next page for additional authors

Recommended Citation

Araujo-Betancor, S., Knigge, C., Long, K., Hoard, D., Szkody, P., Rodgers, B., Krisciunas, K., Dhillon, V., Hynes, R., Patterson, J., & Kemp, J. (2003). The system parameters of DW Ursae Majoris. *Astrophysical Journal, 583* (1 I), 437-445. https://doi.org/10.1086/345098

System Parameters of DW Ursae Majoris[1]

S. Araujo–Betancor, C. Knigge

Department of Physics & Astronomy. University of Southampton, Southampton SO17 1BJ, UK

K. S. Long

Space Telescope Science Institute, Baltimore MD 21218, USA

D. W. Hoard

SIRTF Science Center, IPAC, California Institute of Technology, Pasadena CA 91125, USA

P. Szkody, B. Rodgers[2] & K. Krisciunas[3]

Department of Astronomy. University of Washington, Seattle WA 98195, USA

V. S. Dhillon

Department of Physics & Astronomy. University of Sheffield, Sheffield S3 7RH, UK

R. I. Hynes

Department of Physics & Astronomy. University of Southampton, Southampton SO17 1BJ, UK

J. Patterson & J. Kemp[4]

Department of Astronomy. Columbia University, New York NY 10027, USA

ABSTRACT

We present new constraints on the system parameters of the SW Sextantis star DW Ursae Majoris, based on ultraviolet (UV) eclipse observations with the *Hubble Space Telescope*. Our data were obtained during a low state of the system, in which the UV light was dominated by the hot white dwarf (WD) primary. The duration of the WD eclipse allows us to set a firm lower limit on the mass ratio, $q = M_2/M_1 > 0.24$; if $q < 1.5$ (as expected on theoretical grounds) the inclination must satisfy $i > 71°$. We have also been able to determine the duration of WD ingress and egress from our data. This allows us to constrain the

masses and radii of the system components and the distance between them to be $0.67 \leq M_1/M_\odot \leq 1.06$, $0.008 \leq R_1/R_\odot \leq 0.014$, $M_2/M_\odot > 0.16$, $R_2/R_\odot > 0.28$ and $a/R_\odot > 1.05$. If the secondary follows Smith & Dhillon's mass-period relation for CV secondaries, our estimates for the system parameters become $M_1/M_\odot = 0.77 \pm 0.07$, $R_1/R_\odot = 0.012 \pm 0.001$, $M_2/M_\odot = 0.30 \pm 0.10$, $R_2/R_\odot = 0.34 \pm 0.04$, $q = 0.39 \pm 0.12$, $i = 82^\circ \pm 4^\circ$ and $a/R_\odot = 1.14 \pm 0.06$.

We have also obtained time-resolved I- and K-band photometry of DW UMa during the same low state. Using Bessell's spectral-type vs $(I-K)$ color calibration, we estimate the spectral type of the donor star to be $M3.5 \pm 1.0$. This latter result helps us to estimate the distance towards the system via Bailey's method as $d = 930 \pm 160$ pc.

Finally, we have repeated Knigge et al.'s WD model atmosphere fit to the low-state UV spectrum of DW UMa in order to account for the higher surface gravity indicated by our eclipse analysis. The best-fit model with surface gravity fixed at $\log g = 8$ has an effective temperature of $T_{\rm eff} = 50,000 \pm 1000$ K. The normalization of the fit also yields a second distance estimate, $d = 590 \pm 100$ pc. If we adopt this distance and assume that the mid-eclipse K-band flux is entirely due to the donor star, we obtain a second estimate for the spectral type of the secondary in DW UMa, $M7 \pm 2.0$. After discussing potential sources of systematic errors in both methods, we conclude that the true value for the distance and spectral type will probably be in between the values obtained by the two methods.

Subject headings: stars: binaries: close – stars: binaries: eclipsing – stars: fundamental parameters (masses, radii) – stars: individual: DW UMa - stars: novae, cataclysmic variables – ultraviolet: stars

---

[1]Based on observations with the NASA/ESA Hubble Space Telescope (HST), obtained at the Space Telescope Science Institute (STScI), which is operated by the Association of Universities for Research in Astronomy, Inc., under NASA contract NAS5-26555, and with the Apache Point Observatory (APO) 3.5m telescope, which is owned and operated by the Astrophysical Research Consortium (ARC).

[2]Present address: Gemini Observatory, AURA/Chile, P. O. Box 26732, Tucson AZ 85726, USA

[3]Present address: CTIO, 950 N. Cherry Ave, Tucson AZ 85719, USA

[4]Also Joint Astronomy Centre, University Park, 660 North A'ohoku Place, Hilo HI 96720, USA.

1. Introduction

Nova-likes (NLs) are a subgroup of cataclysmic variables (CVs) in which a late-type main sequence secondary loses mass onto a white dwarf (WD) primary via Roche lobe overflow. If the WD does not have a strong magnetic field, the transferred matter forms an accretion disk with a bright spot where the stream of matter hits the disk. Unlike the more commonly known dwarf nova type CVs, NLs do not undergo quasi-periodic outbursts. They are instead characterized by a high, steady accretion rate which prohibits the disk instability mechanism responsible for the dwarf nova outbursts. However, some NLs with periods between 3-4 hrs also exhibit low states during which mass transfer from the secondary and/or accretion onto the WD decreases or shuts off completely. The reason for the low states is uncertain; one possibility is that they are related to magnetic activity of the secondary star (see Hessman, Gänsicke & Mattei 2000). Supporting this theory is the fact that the orbital period of these systems is very close to the upper edge of the CV period gap between 2-3 hrs. The absence of CVs in this region of the orbital period distribution, is believed to occur as a consequence of a change in the internal structure of the secondary. More specifically, it is thought that at $P_{\rm orb} \approx 3$ hrs, the secondary becomes fully convective and magnetic braking ceases to be the main mechanism by which angular momentum is removed from the system. As a result, the secondary loses contact with its Roche lobe and mass transfer ceases. Gravitational radiation takes over as the dominant, but less efficient, angular momentum loss mechanism. At $P_{\rm orb} \approx 2$ hrs the orbit has shrunk enough for the secondary to re-establishes contact, and mass transfer resumes. For a thorough review of CVs refer to Warner (1995).

The subject of our paper, DW Ursae Majoris, is an eclipsing CV with a period of $P_{\rm orb} = 3.28$ hrs and belongs to a subclass of NLs called SW Sextantis stars (Thorstensen et al. 1991). SW Sex systems are grouped together because they exhibit several unusual properties: (a) they are often eclipsing systems with orbital periods of 3-4 hrs; (b) their continuum eclipses are more V-shaped (as opposed to U-shaped) than those of other NLs; (c) their optical emission lines are single-peaked, instead of double-peaked (as expected for high-inclination, disk-formed lines); (d) their Balmer and HeI lines remain largely unobscured during primary eclipse, but display absorption events at the opposite orbital phase; (e) the radial velocity curves derived from their optical emission lines lag substantially behind the phase one expects from the WD on the basis of eclipses. Several models have been put forward to account for the SW Sex stars, and although each is capable of explaining a subset of the SW Sex behavior, none has so far been able to explain all the features listed above (e.g. Knigge et al. 2000 and references therein).

One reason for our poor understanding of the SW Sex phenomenon is the scarcity of reliable system parameters for members of this class. This scarcity is a direct consequence of

the defining SW Sex characteristics. More specifically, radial velocity studies of SW Sex stars are of limited value, given the ubiquitous and significant phase lags seen in the radial velocity curves of these systems. Eclipse studies have been similarly unsuccessful, since WD contact points are not evident in the V-shaped eclipse light curves of SW Sex stars (perhaps because the disks are self-occulting; Knigge et al. 2000). Also, the high accretion rates exhibited by these systems during normal states cause the late-type main sequence secondary to be invisible against the glare of the WD and/or accretion disk.

The goal of this paper is to improve on this situation by deriving a set of reliable system parameters for DW UMa. This is possible because a recent *Hubble Space Telescope* (HST) observation of the system found DW UMa in a deep low state, during which the WD dominated the ultraviolet (UV) light. This is the second, in a series of papers, describing these observations. The first, Knigge et al. (2000), dealt with the low-state UV spectrum. Here we analyze the time-resolved behavior around the eclipse and discuss I- and K-band photometry obtained during the same low state. The remainder of this article is organized as follows: In section 2, we describe the HST and ground-based observations and their reduction. Next, in section 3, we discuss our determination of the contact phases describing the eclipse of the WD by the secondary. In section 4, we use the contact phases an other information to determine the parameters of the binary system and its constituents. Then, in section 5, we calculate estimates for the distance to DW UMa and for the spectral type of the donor star in two different ways: using our I- and K-band photometry and re-fitting the Knigge et al.'s (2000) WD model atmosphere to the low-state UV spectrum of DW UMa. Finally, in section 6, we discuss our results and compare the system parameters we have derived to those previously reported for DW UMa.

2. Observations

The observations of DW UMa with the HST *Space Telescope Imaging Spectrograph* (STIS), took place on 1999 January 25 UT and covered just over two complete cycles of DW UMa's 3.28 hrs orbital period. DW UMa is in HST's continuous viewing zone (CVZ), so we were able to observe the system almost continuously, with only 3 short ($\simeq 6$ minutes) interruptions between the four separate UV exposures. The instrumental set-up consisted of the $52'' \times 0.2''$ slit, the FUV-MAMA detectors, and the G140L grating. This combination provides a wavelength coverage of $1150 - 1720$ Å at a resolution of $\simeq 1$ Å (FWHM). TIME-TAG mode was used throughout, so that individual photon arrival times were recorded at a sampling rate of 125 μs.

Near-simultaneous optical photometry obtained from the *MDM Observatory* on Kitt

Peak, Arizona, puts DW UMa at $V \simeq 17.6$ around the time of the HST observations. This indicates that the system was in a deep low state at this time ($V \simeq 14.5$ in the high state). Given that the accretion rate must be severely reduced during a low state, the hot WD primary may be expected to dominate the *UV* light in this state. Indeed, Knigge et al. (2000) have already used the same data set to show that the low-state, out-of-eclipse *UV* spectrum of DW UMa is consistent with that of a hot WD. Our *UV* eclipse observations therefore provide us with an unusual opportunity to determine the WD contact phases (and therefore system parameters) of this eclipsing SW Sex star.

For the purpose of the eclipse analysis, we constructed light curves directly from the four TIMETAG files. These files contain a list of the arrival times and detector positions of all recorded photon events, and are therefore ideally suited for short-timescale variability studies. Since we wanted to exclude geocoronal and other strong lines from our light curves, we first determined an approximate linear dispersion relation to relate pixel numbers in the dispersion direction with physical wavelengths. Light curves were then constructed at 1-s time resolution based on all counts recorded in three continuum windows in the dispersion direction, *viz.* 1340 – 1380 Å, 1410 – 1520 Å and 1570 – 1720 Å , and in a 0.36 arcseconds window in the spatial direction. Since we are only interested in determining contact phases, the zero-level of the light curves is irrelevant. We therefore did not carry out any background subtraction on our light curves. The background is, in any case, expected to be negligible: our continuum regions are well separated from geocoronal lines, and dark current contributes only about 7 c/s across the entire FUV-MAMA detector, and therefore less than 0.1 c/s in the small region used for extracting the count rate.

Figure 1 shows the resulting *UV* light curve of DW UMa. Several points should be noted: (i) the count rate at mid-eclipse phases is close to zero, confirming that there is no significant background contribution in our light curves; (ii) there are sharp features in each of the eclipses (especially eclipse 3), which are likely due to ingress and egress of the WD; (iii) the light curves exhibit substantial short-timescale, stochastic variability.

In addition to the HST observations, we have obtained some (near-)infrared *I*- and *K*-band photometry of DW UMa. The *I*-band observations were taken using the MDM 1.3 m telescope on 1999 February 8 and 9 UT, roughly two weeks after the *UV* HST observations. The infrared *K*-band data were obtained on 1999 March 28 UT using the *Apache Point Observatory* (APO) 3.5 m telescope and the GRIMII detector. Near-simultaneous *B*-band photometry (also obtained using MDM) showed that DW UMa was still in its low state during all of these observing runs ($B > 17$). All of the *I*- and *K*-band observations were timed to coincide with eclipses of the system. The mid-eclipse magnitudes of DW UMa in these filters were found to be $I_{\rm kc} = 18.71 \pm 0.14$ (on the Kron-Cousins system) and $K_{\rm ukirt} =$

16.43 ± 0.14 (on the UKIRT system). These values will be used in Section 5 to estimate the spectral type of the donor star and to constrain the distance towards the system via Bailey's (1981) method.

In order to convert the HJD times to orbital phases, we used the ephemeris

$$T_{\rm mid-eclipse} = 2446229.00696(3) + 0.136606499(3)E, \quad (1)$$

where the numbers in parentheses designate the errors on the last digits. This is an updated version (Smith, Dhillon & Marsh 2002) of the ephemeris presented by Dhillon, Jones & Marsh (1994). In practice, we still found an O-C shift of approximately +0.0062 (73 s) with this new ephemeris. This is consistent with that found by Smith et al. (2002) from a high state of DW UMa observed at a similar epoch to ours. Note that our O-C shift, which has been removed in all of the phase-folded light curves shown below, could include a contribution of a few seconds from the uncertainty in the STIS absolute timing (see Long 2000).

3. Method of Measuring the eclipse timings

The phase intervals inside which the WD disappears (ingress) and reappears (egress) from behind the occulting secondary are defined as $\Delta\phi_{\rm wi} = \phi_{\rm w2} - \phi_{\rm w1}$ for ingress, and $\Delta\phi_{\rm we} = \phi_{\rm w4} - \phi_{\rm w3}$ for egress, where $\phi_{\rm w1}$, $\phi_{\rm w2}$, $\phi_{\rm w3}$ and $\phi_{\rm w4}$ are the WD contact phases (c.f. Figure 2). The half-flux phases within each of these intervals, $\phi_{\rm wi}$ and $\phi_{\rm we}$ respectively, are the phases at which half of the light from the compact object is eclipsed. The full-width at half out-of-eclipse intensity is then defined as $\Delta\phi = \phi_{\rm we} - \phi_{\rm wi}$, or, in units of time, $\Delta{\rm t} = P_{\rm orb}\Delta\phi$.

The WD contact phases were measured using the method described by Wood, Irwin & Pringle (1985). Figure 3 illustrates this procedure carried out on eclipse 3. The light curve is smoothed with a median filter of width 11 s. The amount of filtering chosen is a compromise between the desire to reduce the noise (Poisson plus intrinsic variability) and the need to retain the most rapid changes in the eclipse. The smoothed light curve is differentiated numerically to enhance regions of sharp brightness variations. The derivative light curve is then smoothed by applying a mean filter of width equal to the expected value for the times of ingress and egress of the WD (43 s). The largest negative and positive peaks after application of the mean filter indicate the location of the mid-points of ingress and egress respectively. The width at half-peak intensity of these features gives a rough estimate of their duration. A spline function is fitted to the derivative omitting those points inside the estimated ingress and egress intervals. This last step is carried out to account for the contribution (if any) of the extended and slowly varying eclipse of the disk. The fitted function is then subtracted

from the derivative, and the result is smoothed with a median filter of width equal to the median filter used in the first part of the reduction. The contact phases are located by identifying the points where the resultant derivative departs from zero.

The main difficulty in identifying the WD contact phases is the presence of stochastic variability on timescales that are only slightly longer than the duration of WD ingress/egress. Figures 1 and 2 show that this type of variability severely limits our ability to determine WD contact phases for eclipses 1 and 2, in particular. We therefore did not use these two eclipses for measuring the contact points, but only to provide qualitative checks on the contact phases determined from eclipse 3. Figure 2 confirms that the contact phases derived from eclipse 3 are indeed consistent with eclipses 1 and 2. The final value for the duration of the ingress/egress of the WD is $\Delta\phi_{\rm wd} = (\Delta\phi_{\rm wi} + \Delta\phi_{\rm we})/2$. In units of time, this is $\Delta {\rm t}_{\rm wd} = P_{\rm orb}\Delta\phi_{\rm wd}$. Our final estimates of Δt and $\Delta {\rm t}_{\rm wd}$ are listed in the first section of Table 1.

4. Binary parameters

The mass ratio, $q = M_2/M_1$ (M_1 and M_2 are the masses of the WD and secondary, respectively), and inclination, i, of the system can be constrained by considering the eclipse of a point source by a Roche-lobe-filling secondary. More specifically, the observed eclipse duration ($\Delta\phi$) defines a unique relation between q and i. We calculated this relation by using a method similar to Chanan, Middleditch & Nelson (1976). Following their Figure 1, we define a spherical coordinate system centered on the WD, in which the direction vector (θ,ϕ) = (90°,0°) points towards the centre of the secondary. The main idea is to consider the intersection of the secondary's Roche lobe and the plane $\phi = \Delta\phi/2$. This reduces the problem to finding the minimum value of θ along the curve defined by this intersection. For each q, this minimum value is then just the inclination i that produces an eclipse of width $\Delta\phi$. The method requires the critical value of the Roche potential. This is calculated by using the fact that the net effective force vanishes at the inner Lagrangian point; $\partial\psi/\partial r = 0$ at L_1, where ψ is the effective potential. The q vs i relation for our measured $\Delta\phi$ is shown in Figure 4.

The mean duration of the ingress and egress features of the eclipse ($\Delta\phi_{\rm wd}$), together with the calculated numerical relation $i = f(q, \Delta\phi)$, can be used to constrain the remaining binary parameters. In practice, we use the full Roche lobe geometry of the secondary to obtain the radius of the spherical compact primary. For each (i, q) pair, our algorithm computes the radius of the WD scaled to the binary separation, R_1/a, that successfully reproduces the observed value for $\Delta\phi_{\rm wd}$. The WD is assumed to be fully visible; this is appropriate here,

since there is no evidence for an optically thick disk in the low state.

Kepler's third law, which defines the binary separation, a,

$$a = \left(\frac{G}{4\pi^2}\right)^{1/3} M_1^{1/3} \, (1+q)^{1/3} \, P_{\rm orb}^{2/3}, \tag{2}$$

is then combined with a theoretical WD mass-radius relation to yield a definite WD mass, M_1, for each q. The inset in Figure 5 shows the resulting constraints on the component masses for a wide range of mass ratios.

Finally, we use Eggleton's (1983) approximation

$$\frac{R_2}{a} = \frac{0.49 q^{2/3}}{0.6 q^{2/3} + \ln\left(1 + q^{1/3}\right)}. \tag{3}$$

to estimate the volume-averaged radius of the secondary, R_2.

The theoretical WD mass-radius relation that we use was taken from Panei, Althaus & Benvenuto (2000) and describes hot ($T_{\rm eff} = 50,000$ K) CO-core WDs with a relatively massive, non-degenerate hydrogen envelope ($M_{\rm env}/M_1 = 10^{-5}$). The effective temperature adopted here is close to the value (46,000 K) inferred by Knigge et al. (2000) from a WD model atmosphere fit. For reference, the spectrum analyzed by Knigge et al. (2000) was constructed from the time interval between eclipses 2 and 3, when the count rate was high and relatively stable. We used a slightly higher temperature here, because our analysis indicates a higher surface gravity ($\log g$). More specifically, preliminary parameters inferred with a $T_{\rm eff} = 46,000$ K mass-radius relation yielded WD parameters corresponding to $\log g \simeq 8$. As discusses in more detail in Section 5, we then refit the low-state UV spectrum with this new gravity estimate and obtained a new temperature estimate of $T_{\rm eff} = 50,000$ K. We note that the systematic errors associated with the presence or absence of a hydrogen envelope and with errors in temperature up to at least 10,000 K are smaller than the random errors resulting from observational uncertainties. Hence, the iteration process does not change the parameter values substantially, but merely improves their internal consistency.

At this stage, we can already place useful constraints on most of the system parameters, which are listed in the second section of Table 1. These constraints are only based on the eclipse geometry and the theoretical WD mass-radius relationship and are therefore particularly robust. If the mass ratio is made to satisfy $q < 1.5$ (see Figure 5), as required for stable mass-transfer from any main-sequence secondary (Politano 1996; de Kool 1992), the constraints are tightened, as shown in the third section of Table 1.

If we are willing to assume that the secondary star is "typical" for a CV with DW UMa's orbital period, we can tighten our constraints even further by using Smith & Dhillon's

(1998) mass-period relationship for CV secondaries. The resulting estimate for the mass of DW UMa's secondary is $M_2/M_\odot = 0.3 \pm 0.1$, where the error is based on the rms scatter quoted by Smith & Dhillon (1998) for this relationship. The effect of this M_2 constraint on M_1 is shown in Figure 5. The corresponding estimates for all system parameters are listed in the fourth section of Table 1.

5. Spectral Type and Distance

Distances for CVs can be estimated via Bailey's (1981) method. This is based on the fact that the K-band surface brightness, $S_{\rm K}$, is only a weak function of spectral type among isolated, late-type, main-sequence stars. The definition of $S_{\rm K}$ is

$$S_{\rm K} = K + 5 - 5\log d + 5\log R_2 \tag{4}$$

where K is the star's K-band magnitude, R_2 is its radius (in solar units) and d is its distance (in parsecs). The most recent calibration of $S_{\rm K}$ against $(V-K)$ color for late-type stars is due to Beuermann (2000)

$$S_{\rm K} = 2.98 + 0.264(V - K_{\rm cit}). \tag{5}$$

In this equation, V is the usual Johnson waveband, and K is on the CIT system. Our own K-band observations are on the UKIRT system, but according to Leggett (1992), $K_{\rm cit} = K_{\rm ukirt}$. By combining Equations 4 and 5, the distance towards a CV can be determined.

In the case of DW UMa, we have an estimate of the mid-eclipse K-band magnitude obtained during a low-state, i.e., at a time when any WD and disk contribution should be relatively small. This estimate – $K_{\rm ukirt} = 16.43 \pm 0.14$ (Section 2) – should therefore be quite close to the true K-band magnitude of the secondary.

In order to determine, $S_{\rm K}$, one needs the $(V-K)$ color of the secondary. In practice, this is difficult to obtain in most CVs, including DW UMa, because the V-band is usually dominated by the WD and/or the accretion disk of the system, and hence the $(V-K)$ color must be estimated from its (known/assumed) spectral type. In our case, although we do not have a V magnitude for the secondary, we do have an estimate – $I_{\rm kc} = 18.71 \pm 0.14$ – of the mid-eclipse I-band magnitude in the low state. We can therefore use the observed $(I-K)$ color to estimate the spectral type of the secondary and use this to predict its $(V-K)$ color.

More specifically, we use the spectral-type vs color calibration presented by Bessell (1991). This calibration uses optical colors (BVRI) on the Kron-Cousins system, but infrared colors (JHKL) on Bessell & Brett's (1988) homogenized system. We therefore used the transformations provided by Bessell & Brett (1988) to transform our $K_{\rm ukirt} = K_{\rm cit}$ to $K_{\rm BB}$ (on

the Bessell & Brett system), although the resulting correction turned out to be insignificant (+0.02). Armed with the $(I_{\rm kc} - K_{\rm BB})$ color of the secondary (Table 2), we then interpolated on Table 2 of Bessell (1991) to estimate the spectral type of the secondary in DW UMa, $M3.5 \pm 1.0$ (to the nearest half-subtype). This may be compared with the spectral type of $M4.2 \pm 0.8$ predicted by Smith & Dhillon's (1998) orbital period-spectral type relation for CV secondaries (the error here corresponds to the rms scatter of the data about their relation). For this spectral type, Bessell (1991) predicts $(V - K) = 5.0 \pm 0.7$, which in turn gives $S_{\rm K} = 4.3 \pm 0.2$. Here, we have dropped the subscript on K, since the differences between the various systems are insignificant compared to the uncertainty on the color.

Having determined both K and $S_{\rm K}$, we can now estimate the distance to DW UMa. We use the secondary's radius derived from the Smith & Dhillon (1998) mass-period relation for CV secondaries and Eggleton's (1983) approximation for the radius, $R_2/R_\odot = 0.34 \pm 0.04$ (Section 4). Solving Equation 4 for d finally yields an estimate $d = 930 \pm 160$ pc (Table 2).

By comparison, Knigge et al. (2000) estimated $d = 830 \pm 150$ pc from the normalization of their fit to the low state UV spectrum and the radius of the WD inferred from their $\log g$. This agrees very well with our own estimate, but this is partly fortuitous since their fit yielded $\log g = 7.60$, whereas our new parameters suggest $\log g \simeq 8$. We have therefore refit the low state UV spectrum with surface gravity fixed at $\log g = 8$. Visually, this new fit is almost indistinguishable from the fit shown in Knigge et al. (2000), with a reduced Chi-squared of $\chi^2_\nu = 1.55$ (up from $\chi^2_\nu = 1.50$). The parameters describing this new fit are listed in Table 3. Combining this with our new estimate of $R_1/R_\odot = 0.012 \pm 0.001$, we obtain a new value for the distance of $d = 590 \pm 100$ pc. If we adopt this distance estimate and assume that the mid-eclipse K-band flux is entirely due to the secondary, we can also obtain a new estimate for the spectral type of the donor star. With $d = 590 \pm 100$ pc, $K_{\rm ukirt} = K_{\rm cit} = 16.43 \pm 0.14$ and $R_2/R_\odot = 0.34 \pm 0.04$, Equations 4 and 5 predict $(V - K) = 8.5 \pm 1.9$. For this color, Bessell (1991) predicts $SpT_2 = M7 \pm 2.0$ (to the nearest half-subtype). If not all of the K-band light is due to the secondary, the spectral type must be even later.

Our two sets of distance and spectral type estimates are only marginally consistent with each other. We therefore briefly consider potential sources of systematic errors in both of the methods we used to obtain them. Most distance estimates based on Bailey's method are, strictly speaking, lower limits, since the observed K-band magnitude may contain residual disk and/or WD contributions (Hoard et al. 2002). In our case, the situation is less clear. This is because our value for d depends on our spectral type estimate, which in turn is based on the observed $(I - K)$ color. But contamination by sources other than the secondary will affect the measured I- and K-band magnitudes differently. Indeed, any reasonable contaminating spectrum will be bluer than that of the secondary, in which case the I-band

would be more contaminated than the K-band. If so, then our measured $(I-K)$ color would be too blue, our spectral type too early and our predicted $(V-K)$ color also too blue. Thus this effect may cause the distance to be *over*-estimated. It is not clear if our estimate for d is affected by these biases, and, if so, which of them dominates.

By contrast, the key assumption in the WD fit is that the observed spectrum is due entirely to a fully visible WD. We first consider the possibility that the observed spectrum actually includes a contribution from another source. If the spectrum of this source is redder than that of the WD, then the true WD spectrum must be (a) bluer and (b) fainter than the observed spectrum. Effect (a) would tend to make our distance estimate too low, because a hotter WD is intrinsically brighter and, for given radius and observed flux, must therefore be further away. Effect (b) would also lead us to underestimate the distance, since the latter scales with observed flux as $F_{\rm obs}^{-1/2}$. Similarly, if the contaminating spectrum is bluer than the WD spectrum (which seems unlikely), then effect (a) above is reversed and would compete with effect (b). Finally, if a significant portion of the WD is obscured, the observed spectrum arises from a projected area that is smaller than πR_1^2. For a given observed flux (and hence a fixed fit normalization $N = 4\pi R_1^2/d^2$), this would imply that our distance estimate is too large.

In principle, we consider the distance estimate based on the WD model fit more direct, and therefore more reliable, than the estimate derived from Bailey's method. However, the spectral type of the secondary we infer from the former estimate seems suspiciously too late by comparison to other CVs with similar orbital periods (Beuermann et al. 1998). On balance, we therefore expect that the true distance and spectral type will turn out to lie between the values suggested by the two methods.

6. Discussion & Conclusions

SW Sex stars display a range of peculiarities that do not seem to fit the standard steady accretion disk model for NLs. There is currently no single agreed-upon explanation for the SW Sex phenomenon. Indeed, no real consensus has been reached about whether SW Sex stars deserve a NL-sub-class label in the first place. Rather, the SW Sex *syndrome* is so widespread (also seen in X-ray binaries; Hynes et al. 2001) that we must consider the possibility that some important element is missing in our standard picture of the accretion flows. Whatever the nature of the SW Sex stars, they may play an important role in CV evolution: with very few exceptions (e.g., BT Mon with $P_{\rm orb} = 8$ hrs; Smith, Dhillon & Marsh 1998), SW Sex stars have orbital periods falling in the 3 – 4 hrs range, just above the period gap.

Reliable system parameters are desperately needed in order to understand the origin of the SW Sex phenomenon. Unfortunately, the very characteristics that distinguish SW Sex stars from other NLs have also prevented us from accurately determining their physical and geometrical parameters. In particular, the phase-shifted radial velocity curves seen in these systems make it very difficult to accurately determine the K-velocities of the component stars (from which other system parameters could then follow). In addition, the high accretion rates exhibited by the SW Sex stars hamper the detection of the individual components of the system since the accretion disk dominates the emission and may even be self-occulting (Knigge et al. 2000). These latter effects are greatly reduced during the sporadic low states displayed by at least some of the SW Sex stars.

In the case of DW UMa, radial velocity studies have been carried out based on both high-state (Shafter, Hessman & Zhang 1988) and low-state (Dhillon at al. 1994; also see Rutten & Dhillon 1994) observations. However, as emphasized by both sets of authors, neither study has provided reliable results. In the former study, significant $(55^\circ - 75^\circ)$ phase lags were seen in all the radial velocity curves from which K_1 was estimated; in the latter study, the radial velocity curve was based on emission lines that clearly arise on the irradiated front face of the secondary (Rutten & Dhillon 1994), and may therefore provide only a lower limit for K_2.

Our HST low state UV observations of DW UMa have provided a rare opportunity to accurately determine the system parameters of an SW Sex star from the eclipses of its WD. This has been possible because the accretion disk contribution is dramatically reduced, revealing the sharp ingress and egress features that mark the WD eclipse. Therefore, we have been able to avoid many of the difficulties associated with radial velocity studies. However, potential sources of systematic errors remain and include (1) our assumption that the WD is entirely unobscured, (2) the application of the mass-period relation for CV secondaries, and (3) the application of the theoretical mass-radius relation for isolated WDs.

As it turns out, the system parameters listed in Table 1 agree reasonably well with the constraints inferred by Shafter et al. (1988) and Dhillon et al. (1994) from radial velocity analyses. However, as argued above, we consider our new estimates to be considerably more reliable, particularly the ones labelled "fundamental" in Table 1. Our estimate of the WD mass ($M_1/M_\odot \simeq 0.77$) is considerably higher than that obtained by Knigge et al. (2000) from their model atmosphere fit to the low state HST UV spectrum ($M_1/M_\odot \simeq 0.5$). Their estimate was based on the surface gravity inferred from the spectral fit and essentially the same mass-radius relation used here but for a WD with $T_{\rm eff} = 46,000$ K (Panei et al. 2000). Given the systematic uncertainties inherent in spectroscopic $\log g$ estimates, we consider our new set of constraints on the WD parameters more reliable.

Both of our distance estimates, $d = 930 \pm 160$ pc (from Bailey's method) and $d = 590 \pm 100$ pc (from the WD model fit), indicate that DW UMa is quite far away. For comparison, Marsh & Dhillon (1997) estimated $d \gtrsim 850$ [450] pc if the secondary is an $M4$ [$M5$] star, based on the absence of clear secondary signatures in their low-state I-band spectroscopy. We note, however, that even though our estimate of $I \simeq 18.7$ for the secondary star is fainter than the (out-of-eclipse) I-band magnitude they actually observed ($I \simeq 18$), it is brighter than the limit of $I > 19.5$ ($< 25\%$) they suggest for the secondary's contribution to their spectrum. If the mid-eclipse I-band flux in our date is due to the secondary, the latter should have contributed roughly half of the I-band flux in their spectrum.

We conclude this paper by reiterating the need for accurate system parameters for the SW Sex stars. Given that most SW Sex stars are high-inclination systems, it is natural to try and exploit this in the way we have done here. However, eclipse analyses based on WD ingress and egress features are usually impossible, since the light from these systems is usually dominated by their (possibly self-occulting) accretion disks. In the case of DW UMa, we have succeeded only because the system was caught in a deep low state. This raises the obvious question whether other SW Sex systems may also exhibit such low states. This would obviously be interesting for its own sake, but would also open a new avenue of attack for determining their system parameters.

A partial answer to this question is already available: of the 14 objects listed as SW Sex stars in the Göttingen Online CV Catalog[5], 5 (including DW UMa) are already classified as VY Scl stars (i.e., nova-like variables that exhibit occasional low states). We therefore advocate a long-term photometric monitoring program of SW Sex stars. This would tell us whether all SW Sex stars are also VY Scl stars and permit us to exploit the low states when they occur.

We are grateful to Leandro Althaus for providing his WD mass-radius relations in electronic form. Support for this work was provided by NASA through grant GO-7362 from the Space Telescope Science Institute (STScI), which is operated by AURA, Inc., under NASA contract NAS5-26555. R.I. Hynes acknowledges support from grant F/00-180/A from the Leverhulme Trust. We would like to thank T. R. Marsh for providing a code for the full Roche lobe geometry analysis. We also wish to thank the referee, J.Thorstensen, for his insightful comments and suggestions.

[5]http://www.cvcat.org

REFERENCES

Bailey J., 1981, MNRAS, 197, 31 MNRAS, 241, 631

Bessell M. S., 1991, AJ, 101, 662

Bessell M. S. & Brett J. M., 1988, PASP, 100, 1134

Beuermann K., Baraffe I., Kolb U. & Weichhold M., 1998, A&A, 339, 518

Beuermann K., 2000, NewAR, 44, 143

Brown T. M., Ferguson H. C., & Davidsen A. F., 1996, ApJ, 472, 327

Chanan G. A., Middleditch J. & Nelson J. E., 1976, ApJ, 208, 512

de Kool, M. 1992, A&A, 261, 188

Dhillon V. S., Jones D. H. P. & Marsh T. R., 1994, MNRAS, 266, 859

Eggleton P. P., 1983, ApJ, 268, 368

Hessman F. V., Gänsicke B. T. & Mattei J. A., 2000, A&A, 361, 952

Hoard D. W., Wachter S., Clark, L. L. & Bowers T. P., 2002, ApJ, 565, 511

Hynes R. I., Charles P. A., Haswell C. A., Casares J., Zurita C. & Serra-Ricart M., 2001, MNRAS, 324, 180

Knigge C., Long K. S., Blair W. P. & Wade R. A., 1997, ApJ, 476, 291

Knigge C., Long K. S., Hoard D. W., Szkody P. & Dhillon, V. S., 2000, ApJL, 539, 49

Leggett S. K., 1992, ApJS, 82, 351

Long C., 2000, STIS Time-Tag Timing, STIS Technical White Paper 00-175, STScI, Baltimore

Marsh T. R. & Dhillon V. S., 1997, MNRAS, 292, 385

Panei J. A., Althaus L. G. & Benvenuto O. G., 2000, A&A, 353, 970

Politano, M. 1996, ApJ, 465, 338

Rutten R. G. M. & Dhillon V. S., 1994, A&A, 288 773

Shafter A. W., Hessman F. V. & Zhang E. H., 1988, ApJ, 327 248

Smith D. A. & Dhillon V. S., 1998, MNRAS, 301, 767

Smith D. A., Dhillon V. S. & Marsh T. R., 1998, MNRAS, 296, 465

Smith D. A., Dhillon V. S. & Marsh T. R., 2002, MNRAS, submitted

Thorstensen J. R., Ringwald F. A., Wade R. A., Schmidt G. D. & Norsworthy J. E., 1991, AJ, 102, 272

Warner B., 1995, Cataclysmic Variable Stars. Cambridge Univ. Press, Cambridge

Wood J. H., Irwin M. J. & Pringle J. E., 1985, MNRAS, 214, 475

Table 1. Parameters inferred from the eclipse analysis of DW UMa.

Parameter	Value
Eclipse measurements	
Δt (s)	969 ± 4
Δt_{wd} (s)	48 ± 3
Fundamental constraints	
q (M_2/M_1)	> 0.24
M_1 $(M_\odot)$	$0.67 \leq M_1 \leq 1.06$
R_1 $(R_\odot)$	$0.008 \leq R_1 \leq 0.014$
M_2 $(M_\odot)$	> 0.16
R_2 $(R_\odot)$	> 0.28
a $(R_\odot)$	> 1.05
With $q < 1.5$	
q (M_2/M_1)	$0.24 \leq q \leq 1.5$
M_1 $(M_\odot)$	$0.67 \leq M_1 \leq 0.96$
R_1 $(R_\odot)$	$0.009 \leq R_1 \leq 0.014$
M_2 $(M_\odot)$	$0.16 \leq M_2 \leq 1.44$
R_2 $(R_\odot)$	$0.28 \leq R_2 \leq 0.62$
a $(R_\odot)$	$1.05 \leq a \leq 1.50$
i (degrees)	> 71
With M_2-P_{orb} relation	
q (M_2/M_1)	0.39 ± 0.12
M_1 $(M_\odot)$	0.77 ± 0.07
R_1 $(R_\odot)$	0.012 ± 0.001
M_2 $(M_\odot)$	0.30 ± 0.10
R_2 $(R_\odot)$	0.34 ± 0.04
a $(R_\odot)$	1.14 ± 0.06
i (degrees)	82 ± 4

Table 2. Parameters inferred from I- and K-band photometry.

Parameter	Value
$(I_{\rm kc} - K_{\rm BB})$	2.3 ± 0.2
Spectral Type	$M3.5 \pm 1.0$
d (pc)	930 ± 160

Table 3. Parameters inferred from the WD model atmosphere fit.

Parameter	Value[a]
$T_{\rm eff}$ (K)	50,000 ± 1,000
$\log g$ ($\log$ cm s^{-2})	8[b]
$v \sin i$ (km s^{-1})	345 ± 86
Z ($Z_\odot$)	0.71 ± 0.14
$N = 4\pi(R_1/d)^2$ (10^{-24})	2.68 ± 0.10 (stat) ± 0.67 (sys)[c]
$E_{\rm B-V}$ (mag)	0.004 ± 0.004
$\log N_{\rm H}$ (cm^{-2})	19.4 ± 0.06
d (pc)	590 ± 100
Spectral Type	$M7 \pm 2.0$[d]

[a]Uncertainties on the fit parameters correspond to 2σ confidence level for one interesting parameter

[b]Fixed value

[c]The systematic error accounts for the uncertainty in the absolute flux calibration of the spectrum and and in the normalization of the models (Brown, Ferguson & Davidsen 1996; Knigge et al. 1997)

[d]This value was calculated assuming the mid-eclipse K-band flux is entirely due to the secondary and adopting $d = 590 \pm 100$ and $R_2/R_\odot = 0.34 \pm 0.04$

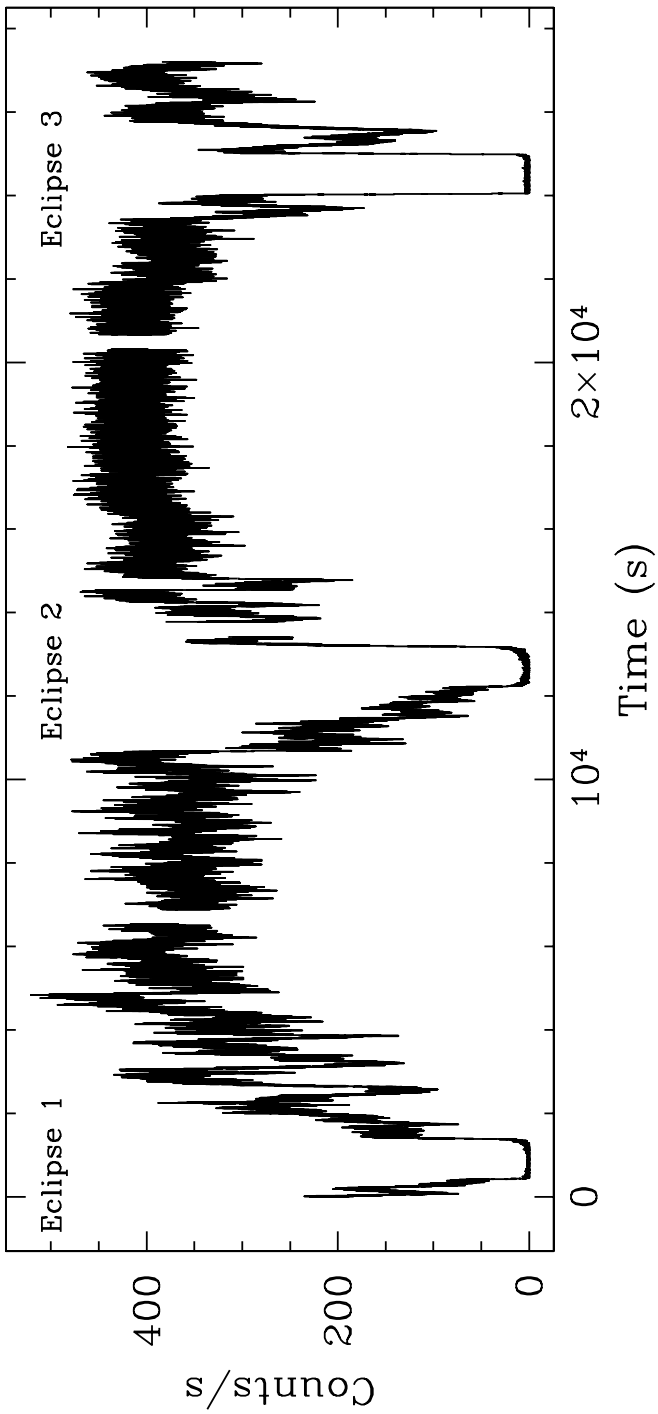

Fig. 1.— DW UMa light curve, with 1 s time resolution, constructed from 3 continuum windows (1340 – 1380 Å, 1410 – 1520 Å and 1570 – 1720 Å) of the HST *UV* spectra. The start time corresponds to 2451203.933 HJD and the total duration of the light curve is 7.55 hrs.

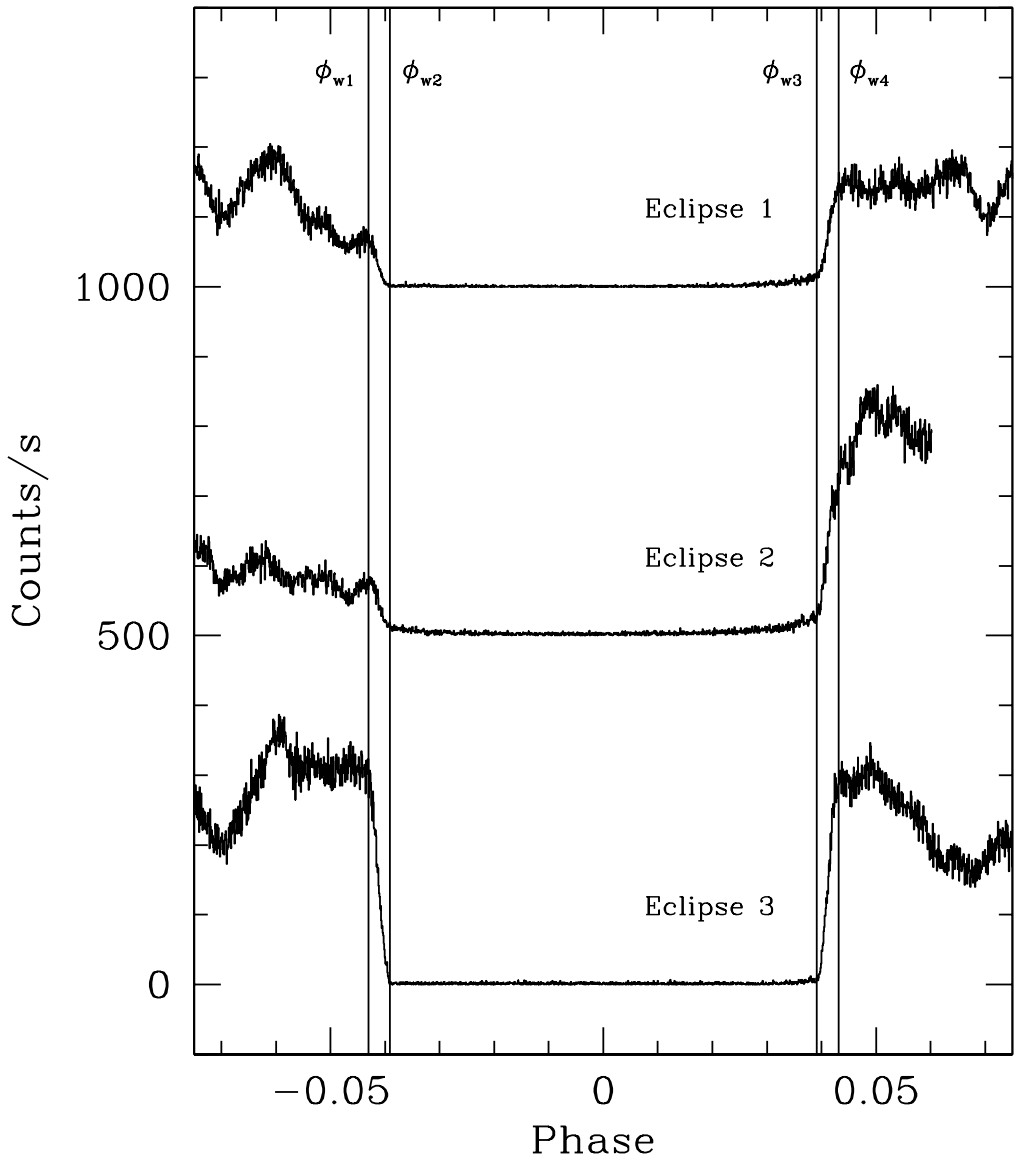

Fig. 2.— The three individual eclipses of Figure 1 plotted against orbital phase. Eclipse 2 and 1 are offset upward by 500 and 1000 counts/s respectively. The vertical lines mark the locations of the contact phases (ϕ_{w1}, ϕ_{w2}, ϕ_{w3} and ϕ_{w4}) inferred from eclipse 3 (see Figure 3).

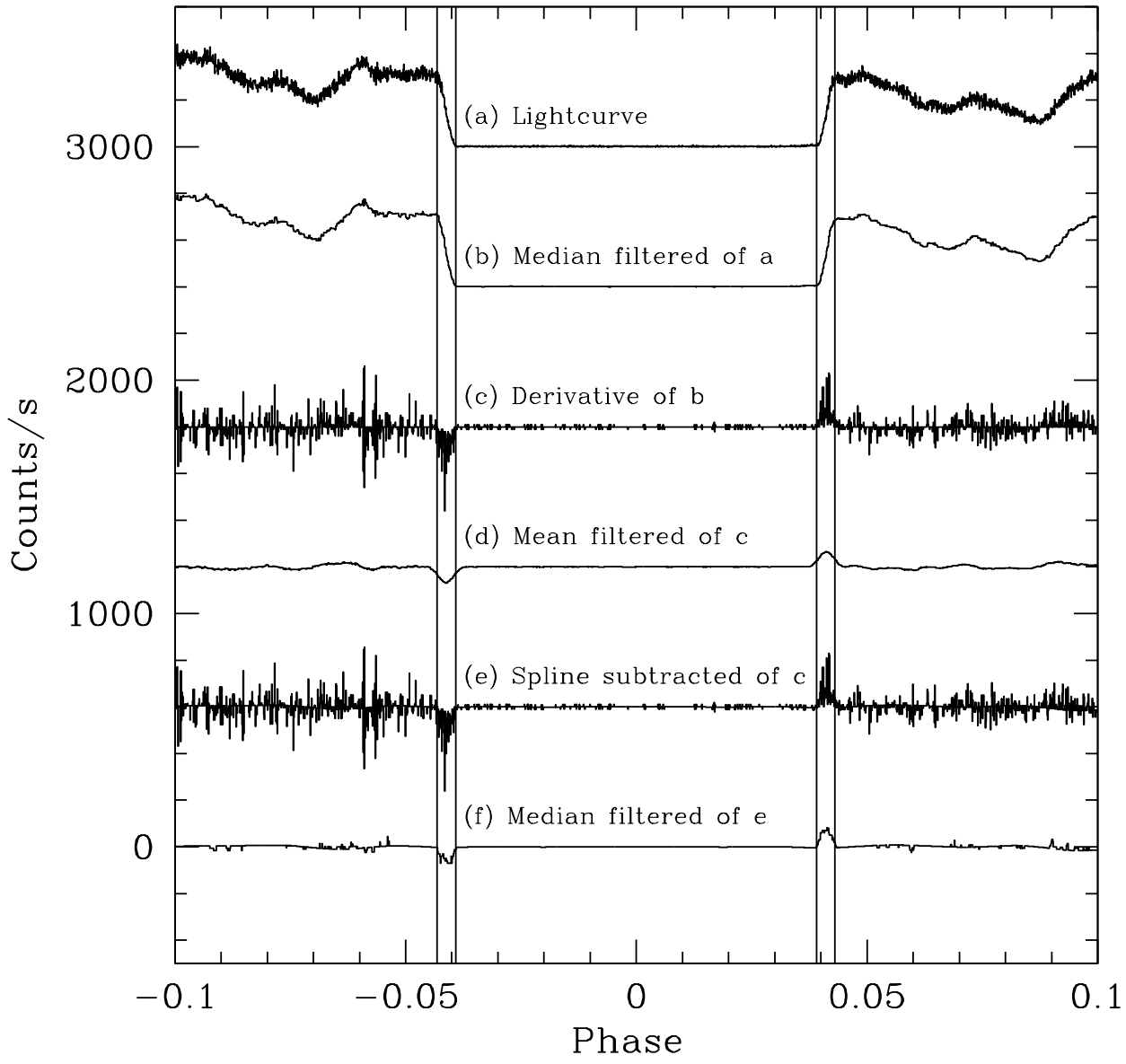

Fig. 3.— Illustration of the method used to obtain the contact phases from eclipse 3 of the light curve of DW UMa. Curves (a) - (e) were successively displaced upward by 600 counts/s each from curve (f). Curves (c), (d), (e) and (f) have been multiplied by a factor of 10 s for clarity. (a) Original light curve with 1 s time resolution. (b) Median-filtered light curve (filter width 11 s). (c) Derivative of the median-filtered light curve. (d) Mean-filtered derivative (filter width 43 s). The highest negative and positive points in this curve indicate the location of the mid-points of ingress and egress respectively, (i.e., $\phi_{\rm wi}$ and $\phi_{\rm we}$). (e) Result of the spline fit and subtraction from the derivative light curve. (f) Median filtered version of (e) (filter width 11 s). The vertical lines represent the measured positions of the contact points $\phi_{\rm w1}$, $\phi_{\rm w2}$, $\phi_{\rm w3}$ and $\phi_{\rm w4}$.

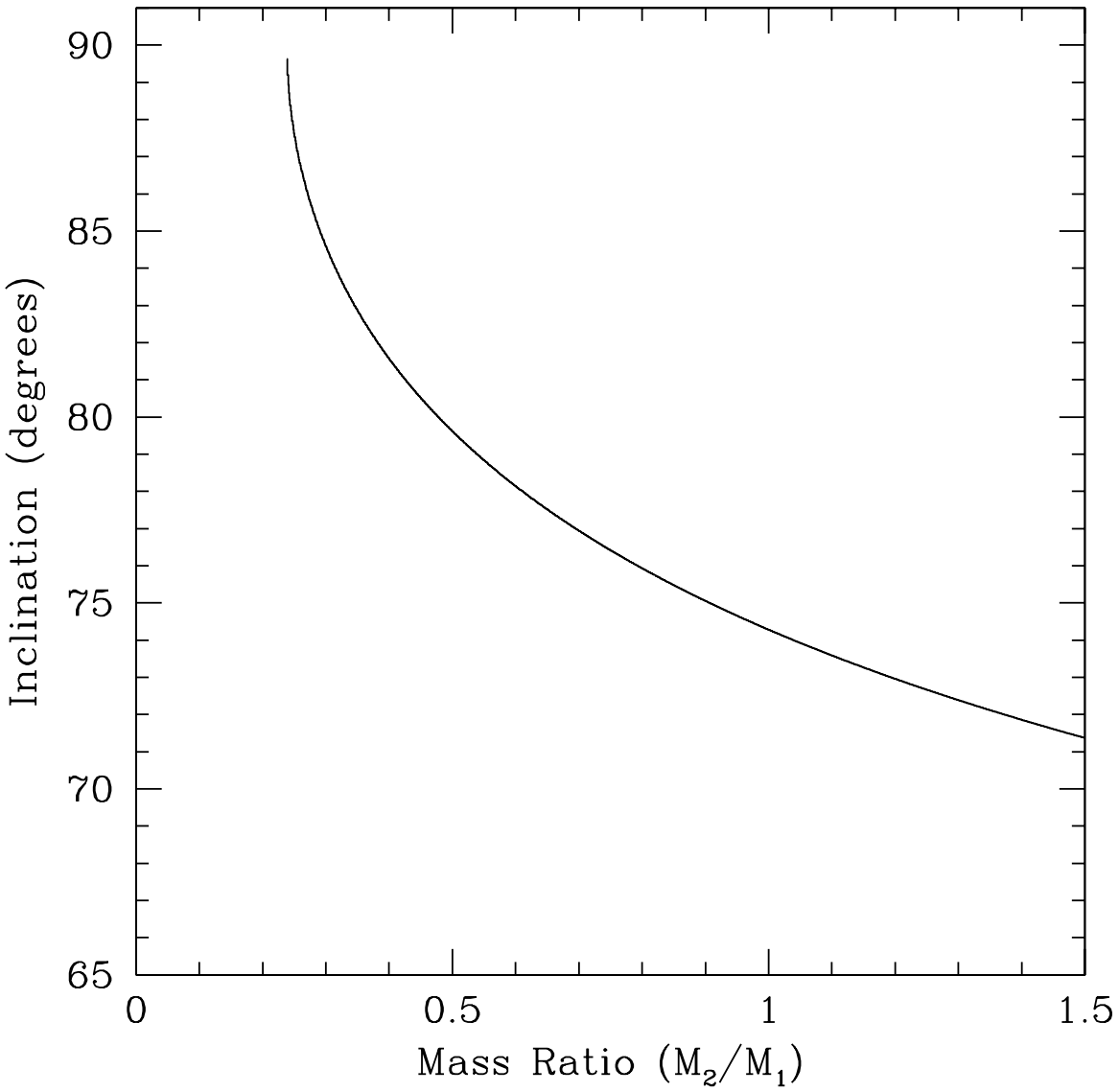

Fig. 4.— Orbital inclination, i, as a function of mass ratio, q. Note that the uncertainty limits on the q vs i relation were not plotted as they were negligible compared to the scale of figure.

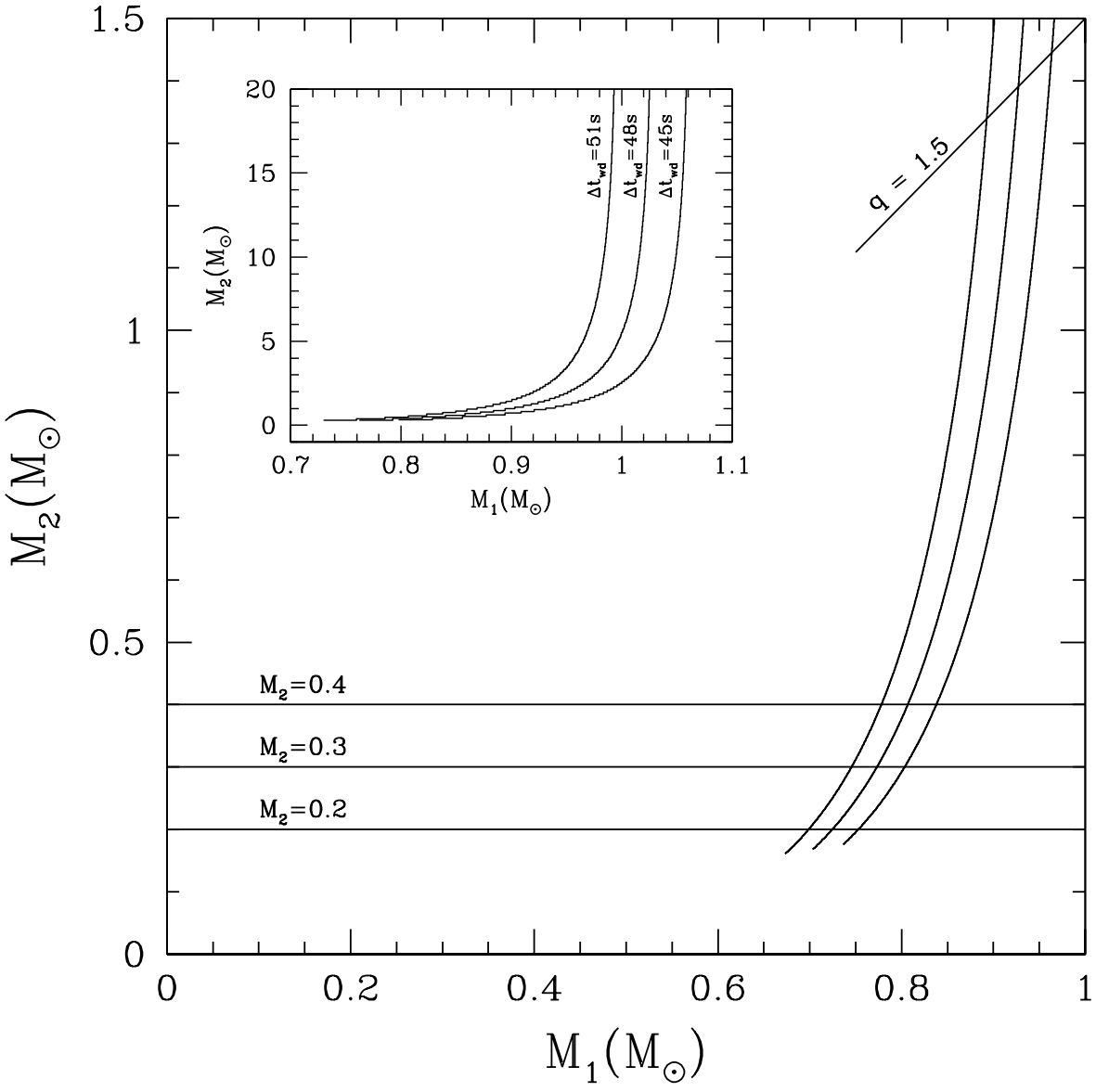

Fig. 5.— Constraints on the component masses of DW UMa. The three curves in both plots correspond to Δt_{wd} = 45 s, 48 s and 51 s. The inset shows a larger range of values for M_2 so that the fundamental upper limits on M_1 can be clearly seen. The $q = 1.5$ line on the main plot shows the upper limits on the component masses based on theoretical grounds (see text). The horizontal lines represent the value of $M_2/M_\odot = 0.3 \pm 0.1$ obtained from the $M_2 - P_{orb}$ relation of Smith & Dhillon (1998). The corresponding value for the mass of the WD is $M_1/M_\odot = 0.77 \pm 0.07$.